Automated Characterization of Normal and Diseased Regions of Calcified Layers in Human Patella from Ultrashort Echo Time (UTE) Imaging on a 3T clinical system.

S. Sinha[1], S. Ahn[2], J. Du[1], U. Sinha[3], A. Takahashi[4], and C. B. Chung[1]

[1]Radiology, University of California at San Diego, San Diego, CA, United States, [2]Biomedical Engineering, University of California at Los Angeles, Los Angeles, CA, United States, [3]Radiology, University of California at Los Angeles, Los Angeles, CA, United States, [4]Global Applied Science Laboratory, GE Healthcare, Menlo Park, CA, United States

Objectives: Tissues with short T2s (~1ms) such as the calcified and deep radial layers of the cartilage are typically invisible on conventional MR images but maybe rendered visible using ultrashort echo time (UTE) imaging. Different pulse sequences and imaging protocol using this relatively new imaging technique need to be compared in the process of optimizing the contrast between normal and diseased regions of the short T2 components of the cartilage. To minimize the intra-observer and inter-exam variability with these different imaging schemes and provide an adjuvant modality for diagnosis by the radiologist, a semi-automated method of classifying the deep layers of cartilage and subchondral bone on UTE images into normal and diseased regions was developed.

Materials and Methods: Images of 6 human disarticulated patella were acquired on a 3T GE system with a 3" surface coil, with a TE/TR/FA=12us/500ms/60°, 512x512 projection reconstructed matrix, 2mm Sl.Thk, non-fat suppressed UTE sequence. The following semi-automated algorithm was developed using Matlab. An area of interest was first defined (Fig.1) within this image of the patella. The area of interest was then segmented using active contours without borders algorithm. Amongst the several contours that generally resulted, the correct one (subchondral bone-calcified layer interface) was selected by the user clicking on both ends of the contour. The contour points then were smoothed (3x1 or 5x1 filters) and fitted with a B-spline (Fig. 2). In the detected contour of the calcified layer, perpendicular lines (normal vectors, Fig. 3) were generated at regular intervals. Intensity profiles of each of these normal vectors were generated (Fig. 4 shows for Profile 1 red, and 5, blue of Fig.3). The UTE images were also visually graded by two experienced musculoskeletal radiologists, and a subset of the profiles in the histologically proven areas of normal cartilage chosen as "the normal template" against which to compare the rest of the profiles. Each of the other profiles were then (i) shifted along the X-axis (Fig. 5), to maximize an initial cross-correlation coefficient with the reference profile, (i.e. their mid-points were at the same X-axis point, Fig. 5), (ii) sub-sampled to ~25 points, (iii) fitted to the first 3 Fourier coefficients after Fourier series expansion of the profile, using the equations given in the inset, and (iv) the correlation coefficient was calculated between the normal and each of the test profiles, after both were fitted and sub-sampled. This coefficient was finally used to classify between normal and diseased calcified cartilage. Finally, the number of points along the contour of the calcified layer that were correctly classified by the semi-automated method (i.e. in agreement with the radiologists' findings) in these 6 patella was determined as a percentage of the total points.

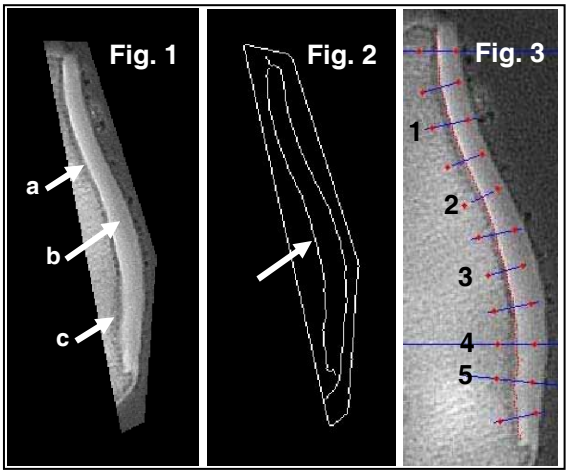

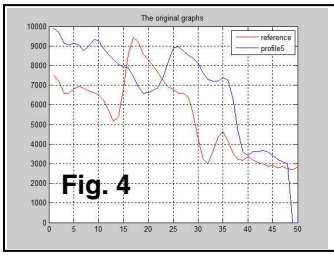

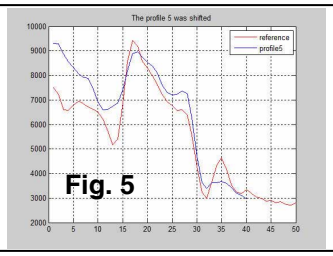

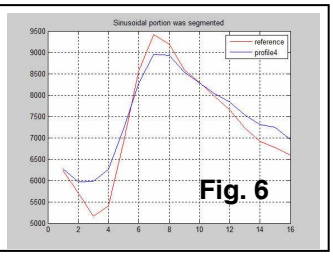

$$f(n) = a_0 + \sum_{m=1}^{\infty} [a_m \cos(m\frac{2\pi}{N}n) + b_m \sin(m\frac{2\pi}{N}n)], \text{ where, } a_0 = \frac{1}{N}\sum_{n=1}^{N} f(n),$$

$$a_m = \frac{2}{N}\sum_{n=1}^{N} f(n)*\cos(m\frac{2\pi}{N}n), \text{ and, } b_m = \frac{2}{N}\sum_{n=1}^{N} f(n)*\sin(m\frac{2\pi}{N}n)$$

Results and Discussion: The advantage of the active contour algorithm is that it did not require the edges to have sharp intensity gradients and could perform robustly in the presence of diffuse borders, with edges fuzzy from artifacts, disease or the presence of intensity shading artifacts. The actual contours were not used for characterization; rather the correlation coefficients of the fitted curves of intensity profiles with the normal profile were. For illustrative purposes, the correlation coefficient obtained for Profiles 1, 3, 4 and 5 (Fig.3) were 1.0, 0.959, 0.90 and 0.703 respectively. These corresponded well with the normal (1~.959) versus diseased (~0.7) extent as graded visually by the radiologists. The percent of points correctly classified by our present algorithm was ~82%.

Conclusion: Since this methodology does not depend on the sharpness with which the calcified layer is detected as much as on the fitting of the profiles to the Fourier series and subsequent correlation, this technique has the potential to be an observer- and pulse-sequence invariant method of quantifying the accuracy of diagnosis between normal and diseased calcified regions.